Journal of Membrane Science 403–404 (2012) 121–128

Contents lists available at SciVerse ScienceDirect

Journal of Membrane Science

journal homepage: www.elsevier.com/locate/memsci

Electrochemical performance of membranes based on hydrogenated polynorbornenes functionalized with imide side groups containing sulfonated fluorinated moieties

Arlette A. Santiago[a], Joel Vargas[b], Mikhail A. Tlenkopatchev[c,*], Mar López-González[d,*], Evaristo Riande[d]

[a] Facultad de Química, Universidad Nacional Autónoma de México, CU, Coyoacán, México DF 04510, Mexico
[b] Facultad de Ingeniería, Universidad Autónoma del Carmen, Avenida Central S/N Esq. con Fracc. Mundo Maya, C.P. 24115, Ciudad del Carmen, Campeche, Mexico
[c] Instituto de Investigaciones en Materiales, Universidad Nacional Autónoma de México, Apartado Postal 70-360, CU, Coyoacán, México DF 04510, Mexico
[d] Instituto de Ciencia y Tecnología de Polímeros (CSIC), 28006 Madrid, Spain

ARTICLE INFO

Article history:
Received 18 February 2011
Received in revised form 31 January 2012
Accepted 19 February 2012
Available online 28 February 2012

Keywords:
Ring opening metathesis polymerization
Sulfonated fluorinated polynorbornene dicarboximide
Cation-exchange membrane

ABSTRACT

This work reports the electrochemical characteristics of a new cation-exchange membrane based on a polynorbornene functionalized with substituted dicarboximide side groups, specifically hydrogenated poly(*N*-4-oxybenzenesulfonic acid-2,3,5,6-tetrafluorophenyl-*exo*-*endo*-norbornene-5,6-dicarboximide). A thorough study on the electrochemical characteristics of the membrane involving osmotic flow, electromotive forces of concentration cells and proton conductivity is reported. This work shows that the polymer membrane exhibits a proton conductivity of 2.24 S/m at 30 °C, the same order of magnitude as that reported for Nafion membranes at the same temperature. The proton permselectivity of the membrane is also discussed.

1. Introduction

Ion-exchange membranes have received considerable attention due to their successful applications in desalination of sea-water and brackish-water, treatment of industrial effluents, concentration or separation of food and pharmaceutical products containing ionic species, manufacture of high purity basic chemical products, etc. [1,2]. Although in the last decades reverse osmosis displaced electrodialysis for water desalination, the interest in ion-exchange membranes is still growing due to the use of these materials as solid electrolytes in low temperature fuel cells.

Whatever the applications of ion-exchange membranes are, these materials should exhibit high conductance, high permselectivity, low free-diffusion of ionic species, low osmotic flow, low electro-osmosis, low fuel crossover, good mechanical properties and high chemical stability. Great efforts have been made to predict the conductivity of cation-exchange membranes in the acid form using Molecular Dynamics techniques [3–6], but the screening of a large number of polyelectrolytes having different chemical structures is still the better procedure to increase the chances of finding specific membranes with suitable transport properties, good chemical stability and good mechanical properties. In this context, cation-exchange membranes based on perfluorinated polymers, polyimides, polyetherketones, polysulfones, polyphosphazenes, etc., have been prepared and their electrochemical characteristics, especially conductivity, have been investigated [7]. Pursuing in this line of research and as a result of the facilities offered by norbornene monomers to be functionalized, membranes have been prepared from polynorbornene functionalized with dicarboximide side groups in which the hydrogen of the imide group is replaced by adamantyl, phenyl, cyclohexyl, pentafluorophenyl, etc., moieties. The performance of functionalized norbornene membranes in gas transport was thoroughly studied [8–10]. Taking into account these antecedents and searching for new ion-exchange membranes, a study was undertaken focused on the preparation of cation-exchange membranes based on modified polynorbornenes.

In an earlier work, the hydrogenation of poly(*N*-phenyl-*exo*-*endo*-norbornene-5,6-dicarboximide) and further sulfonation of the polymer in solution with acetyl sulfate has been reported [11]. A drawback of these membranes is that the sulfonation

* Corresponding authors. Tel.: +52 5556224586; fax: +52 5556161201.
E-mail addresses: tma@servidor.unam.mx (M.A. Tlenkopatchev), mar@ictp.csic.es (M. López-González).

0376-7388/$ – see front matter © 2012 Elsevier B.V. All rights reserved.
doi:10.1016/j.memsci.2012.02.034

procedure does not guarantee a uniform sulfonation of the phenyl groups and even it can produce degradative processes in the polymer chains. In order to circumvent these difficulties, efforts were focused on the development of sulfonation processes of membranes based on functionalized polynorbornenes using mild conditions. This task was recently achieved in our laboratories by successfully replacing the fluorine atom in position 4 of the phenyl group of hydrogenated poly(*N*-pentafluorophenyl-*exo-endo*-norbornene-5,6-dicarboximide) by 4-oxybenzenesulfonic acid [12]. The presence of fluorine atoms in the polyelectrolyte side-chains decreases attractive intermolecular interactions between phenyl groups thus avoiding the molecular piling of the phenyl rings. This behavior is a direct consequence of the high electronegativity of the fluorine atom which severely reduces the polarizability of the C^{ar}—F bond and as a result the formation of non permanent or flitting dipoles which are the basis of the London dispersion forces [13]. It should be noted that earlier studies on gas transport in polynorbornene based membranes showed that fluorinated moieties in the polymer chains cause a significant increase in gas permeability as a consequence of the decrease in intramolecular interactions [14]. Moreover the permeability seems to decrease when the hybridization of the C atom in the C—F bonds passes from sp^2 to sp^3 [10]. In view of these antecedents, it is important to investigate whether the presence of fluorine atoms in acid membranes based on modified polynorbornene electrolytes favors the formation of percolation paths for proton transport, a fact that would be reflected in the enhancement of the conductivity of the membranes. To test this assumption, a new cation-exchange membrane was cast from solutions of hydrogenated poly(*N*-4-oxybenzenesulfonic acid-2,3,5,6-tetrafluorophenyl-*exo-endo*-norbornene-5,6-dicarboximide). The conductivity of the membrane in the acid form, equilibrated with water, was measured at different temperatures and the results were interpreted in terms of the diffusion of protons in the membrane. The permselectivity of the membrane to protons was estimated from the electromotive forces of concentration cells containing hydrochloric acid as electrolyte. The acronym used for the polymeric acidic membrane was P5FNDIHS and the structural unit of the chains is shown in Fig. 1.

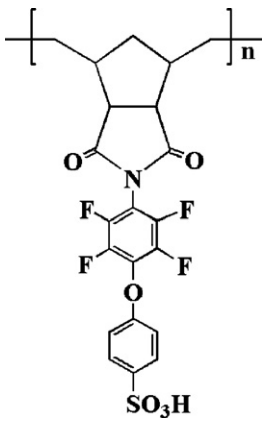

Fig. 1. Acid form structural unit of hydrogenated–sulfonated poly(*N*-pentafluorophenyl-*exo-endo*-norbornene-5,6-dicarboximide) (P5FNDIHS).

2. Experimental part

2.1. Synthesis of the monomer

By reaction of norbornene-5,6-dicarboxylic anhydride (NDA) with 2,3,4,5,6-pentafluoroaniline an amic acid (AA) is obtained which further treated with anhydrous sodium acetate/acetic anhydride produces the monomer *N*-pentafluorophenyl-*exo-endo*-norbornene-5,6-dicarboximide (5FNDI) (see Scheme 1). More details of the synthesis are given elsewhere [12].

2.2. Polymerization

Polymerization of 5FNDI was carried out by ring opening metathesis polymerization (ROMP) (Scheme 1). The reaction was performed at 45 °C for 2 h in glass vials, under nitrogen atmosphere. The polymerization was terminated by adding ethyl vinyl ether to the reaction medium which was further poured into methanol, solubilized with chloroform containing a few drops of 1 N HCl and precipitated again into methanol. The product was dried in a vacuum oven at 40 °C to constant weight. Then, the polymer was hydrogenated quantitatively at room temperature and 115 bar using a Wilkinson's catalyst (Scheme 2).

2.3. Sulfonation procedure

Hydrogenated poly(*N*-pentafluorophenyl-norbornene-5,6-dicarboximide) (P5FNDIH) (0.5 g, 1.51 mmol), sodium 4-hydroxybenzenesulfonate dihydrate (0.70 g, 3.02 mmol) and potassium carbonate (0.52 g, 3.77 mmol) were mixed in a round flask equipped with a Dean-Stark trap and stirred in 15 mL of solvent (*N*,*N*-dimethylacetamide–toluene 2:1) at 120 °C for 9 h (Scheme 2). Progressive precipitation overtime was observed. The product was then filtered off, washed several times with distilled water and dried in a vacuum oven at 40 °C overnight. The resulting polymer P5FNDIHS, a pale-brown powder, was soluble in DMF and DMSO. Yield: 94%, T_g = 228 °C, T_{d1} = 260 °C (sulfonic group loss), T_{d2} = 430 °C (main chain decomposition).

^{1}H NMR (300 MHz, DMF-d_7): δ (ppm) = 7.80 (2H, s), 7.18 (2H, s), 3.56 (2H, s), 2.73, 2.31, 1.83, 1.58, 1.91.

^{13}C NMR (75 MHZ, DMF-d_7): δ (ppm) = 175.0 (C=O), 145.5, 145.0, 140.4, 139.7, 128.2 (C—O), 115.1, 107.2, 49.0, 43.0.

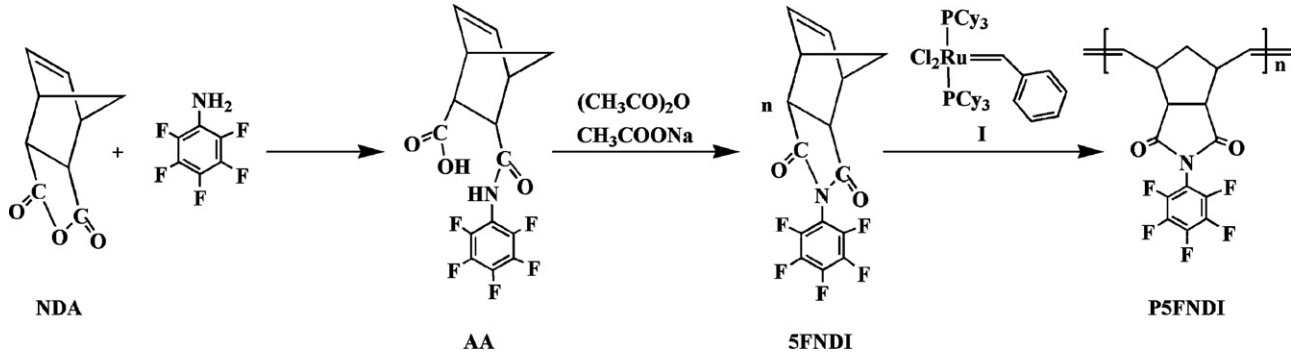

Scheme 1. Monomer synthesis and further polymerization.

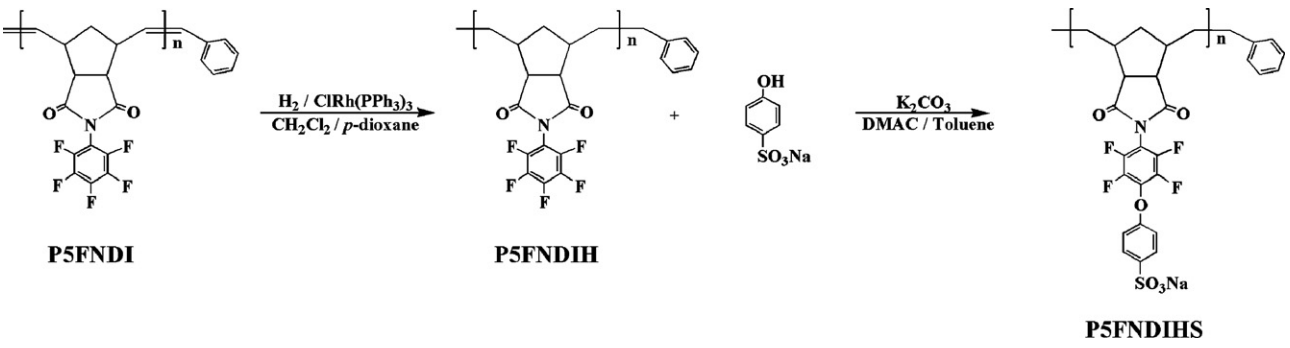

Scheme 2. Synthesis of sulfonated polymer.

^{19}F NMR (300 MHz, DMSO-d_6, ref. TFA [−77 ppm]): δ (ppm) = −141.9, −143.0, −153.1.

FT-IR (thin film, cm^{-1}): 2926 (C—H asym str), 2860 (C—H sym str), 1787 (C=O), 1726, 1636, 1509, 1406, 1356, 1295 (C—F), 1140 (—SO_3H, asym str), 1132, 1039 (—SO_3H, sym str), 981, 833, 698, 561. The acronym for this polymer will be P5FNDIHS.

2.4. Membranes preparation and Atomic Force Microscopy (AFM)

P5FNDIHS membranes (in sodium salt form) were cast respectively from hot *N,N*-dimethylformamide solutions (∼2 wt%) of P5FNDIHS chains in a Teflon mold and dried at 70 °C for 12 h. The films were immersed firstly in stirring methanol at room temperature for 3 h and secondly in deionized water for 1 h in order to remove the residual solvent. Afterwards, the membranes underwent a proton exchange treatment with 1.0 N hydrochloric acid during 12 h. Then, the films were washed repeatedly with deionized water until the rinse water became neutral. Finally, the membranes were dried under a vacuum at 120 °C for 10 h.

The surface morphology of the thin films was observed using tapping mode AFM (Multimode Nanoscope IVa, Digital Instrument/Veeco) under ambient conditions. In tapping mode, the stylus oscillates and touches the sample only at the end of its downward movement. The nominal resonance frequency for the tapping mode was between 265 and 309 kHz with a phosphorous (n) doped Si cantilever which had a spring constant that ranged from 20 to 80 N m^{-1}. The set point in the AFM control program was adjusted to change the contact force between the tip and surface in order to detect the existence of morphologies.

2.5. Density, water uptake and ion-exchange capacity of the membranes

The density of the dry membrane was measured by the flotation method using isooctane as solvent obtaining for this quantity the value of 1.50 g cm^{-3}.

The weighed dry membrane was immersed in distilled water for several hours, removed from the solution, gently blotted with filter paper to remove superficial water and weighed. From the weight of the dry membrane, m_d, and the membrane equilibrated with water, m_w, the water uptake, w_u, in g H_2O/g dry membrane was obtained as $w_u = (m_w/m_d) - 1$. The pertinent result for w_u was 0.617 g cm^{-3}.

The ion-exchange capacity (IEC) of the membrane was measured by immersing the weighed dry membrane in a 1 N HCl solution for 1 h. Then the membrane was removed from the solution, washed several times with distilled water to eliminate the chloride acid absorbed, and finally immersed in a 1 N sodium chloride solution. The protons exchanged in the reaction

$$R\text{–}H + Na^+ \rightarrow R\text{–}Na + H^+ \quad (1)$$

were estimated by titration with a very diluted NaOH solution. The value of IEC in equiv./kg dry membrane was calculated as IEC = VN/m_d where V is the volume in L of the solution of NaOH of normality N (equiv./L) used in the titration and m_d is the mass in kg of the dried membrane. The value obtained for IEC was 1.75 equiv./kg dry membrane, somewhat lower than that estimated from NMR which amounts to 2.06 equiv./kg dry membrane. As a result, the number of moles of water per fixed —SO_3^- group of the membrane are 16.6 and 19.6 according, respectively, to the IEC data obtained by NMR and titration.

2.6. Electromotive forces of concentration cells

Electromotive forces of concentration cells made up of two semi-cells separated by the ion-exchange membrane were measured. The configuration of the cells was Ag|AgCl|HCl solution (c_1)|cation-exchange membrane|HCl solution (c_2)|AgCl|Ag, where c_1 and c_2 are the concentrations of the electrolyte in the left-hand and right-hand compartments of the concentration cells. Notice that the anion of the electrolyte must be reversible with that of the electrodes. The solution in each compartment was kept under strong stirring to minimize the formation of membrane–solution interface layers. The evolution of electromotive force, *emf*, of the cell with time was measured at 25 °C with a 3645-20 Hioki voltage logger, and recorded every second with a 3911-20 communication base apparatus via a PC. The *emf* of the concentration cell was taken as that one at which this quantity reaches a maximum.

2.7. Ohmic resistance measurements

The ohmic resistance of the membrane in the acid form was measured with a Novocontrol BDS system comprising a frequency response analyzer (Solartron Schlumberger FRA 1260) and a broadband dielectric converter with an active sample head. Gold disk electrodes were used in the impedance measurements carried out at several temperatures in the frequency window 4.9×10^{-2} to 3×10^6 Hz. The temperature was controlled by a nitrogen jet (QUATRO from Novocontrol) with a temperature error of 0.1 K during every single sweep in frequency.

2.8. Osmotic measurements

Osmotic flow across the acidic membrane was measured using the configuration: distilled water|acidic membrane|hydrochloric acid solution. Each of the two compartments was equipped with a horizontal capillary of 0.79 mm diameter to measure the liquid flow across the membrane. To decrease interface effects, the liquid in the compartments was strongly stirred with magnetic stirrers. The experiments were carried in the cell immersed in a water thermostat, set at 30 °C.

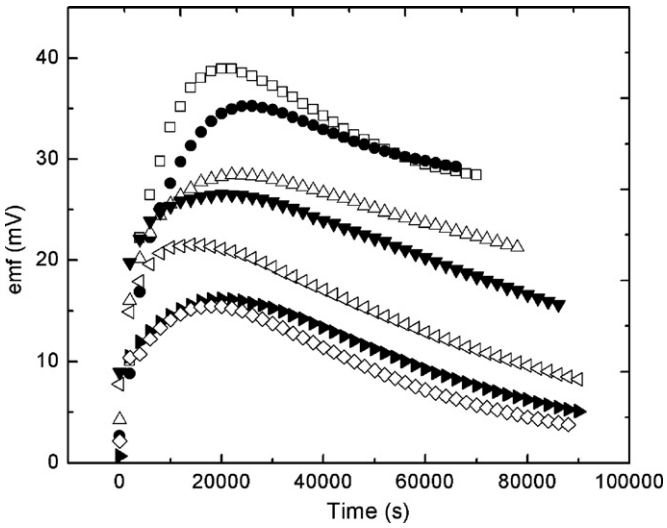

Fig. 2. Evolution of the *emf* of the P5FNDIHS membrane for different c_2/c_1 ratios: (□) 0.01/0.005, (●) 0.02/0.01, (△) 0.1/0.05, (▼) 0.2/0.1, (◁) 0.4/0.2, (►) 0.8/0.4, and (◊) 1.0/0.5.

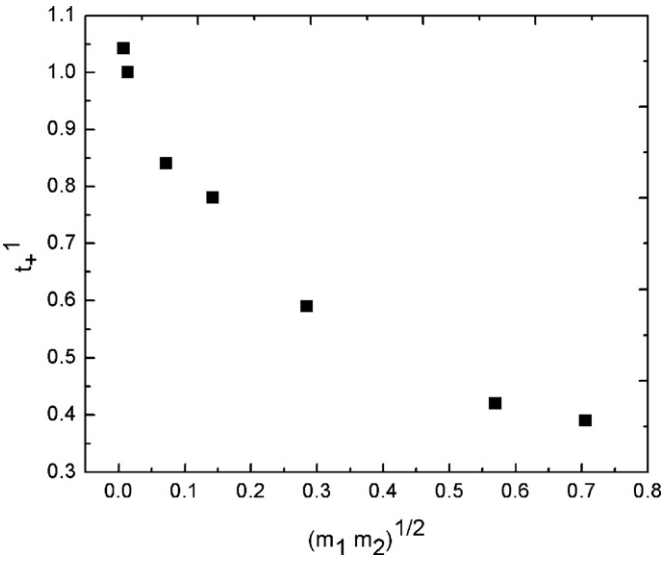

Fig. 3. Variation of the apparent proton transport number with the geometric average of the molality of the solutions flanking the membrane in P5FNDIHS.

3. Results

The variation of the electromotive force, *emf*, of the concentration cell with time for several HCl solutions flanking the membrane is shown in Fig. 2. The ratio between the concentrations of the solutions in the concentrated, c_2, and diluted, c_1, compartments lies in the vicinity of 2. In all cases, prior to each experiment, the membrane was washed several times with distilled water until exhausting the free electrolyte inside the membrane and then was equilibrated with the solution used in the dilute compartment of the concentration cell. An inspection of the evolution of the curves in the figures shows that the *emf* of the concentration cell increases with time needing nearly 3 h in most cases to reach the maximum value and then decreases as time increases. The *emf* at the maximum of the curves was taken as the apparent electromotive force of the concentration cell flanked by electrolyte solutions with concentration c_2/c_1.

The *emf* of a concentration for an electrolyte $A^{z_+}_{\nu^+}B^{z_-}_{\nu^-} \rightarrow \nu^+A^{z_+} + \nu^-B^{z_-}$ is given by [15]

$$emf = \frac{\nu RT}{z_+F}\int_{a_1}^{a_2} t_+(c)d\ln a_\pm = \frac{\nu RT}{F}\int_{a_1}^{a_2} \tau_+(c)d\ln a_\pm \tag{2}$$

where a_1 and a_2 are respectively the activities of the electrolyte solutions in the compartments 1 and 2 of the concentration cell, t_+ and τ_+ ($=t_+/z_+$) are respectively the number of equivalents and moles of cations transported across the membrane by a Faraday of current, F, and $\nu = \nu_+ + \nu_-$ is the total number of moles of ions proceeding from the dissociation of the electrolyte. For monovalent electrolytes, such as HCl, Eq. (2) becomes

$$emf = -\frac{2RT}{F}\int_{a_1}^{a_2} t_+(c)d\ln a_\pm \tag{3}$$

Notice that for monovalent electrolytes, $t_+ = \tau_+$. Since transport numbers depend on the concentration of electrolyte, solution of Eq. (3) requires measuring the $t_+(c)$ profile across the membrane using the Hirthoff method, i.e. determining the variation of concentration of electrolyte in a concentration cell flanked by the electrolyte at the same concentration c after passing a known amount of dc current across the membrane. However, if the concentration ratio c_2/c_1 is 2 or lower, the average transport number of the cation can approximately be estimated as

$$t_+ = \frac{emf}{emf_{\max}} \tag{4}$$

where *emf* is the experimental value of the concentration cell and $emf_{\max}$ can be obtained doing $t_+ = 1$ in Eq. (3), i.e.,

$$emf_{\max} = -\frac{2RT}{F}\ln\frac{a_2}{a_1} \tag{5}$$

Values of the apparent proton transport numbers for different concentrations flanking the membrane are shown in Fig. 3.

The dependence of the osmotic flux on the concentration of the hydrochloric acid in the electrolyte compartment of the osmotic cell for the P5FNDIHS membrane is shown in Fig. 4. The results show that in increasing the concentration of hydrochloric acid from 0.01 N to 1 N, the flux of water increases more than one order of magnitude, specifically from 3.7×10^{-6} cm^3 cm^{-2} s^{-1} to 8.1×10^{-5} cm^3 cm^{-2} s^{-1}.

The response of cation-exchange membranes in acid form to an alternating electric field of angular frequency ω is modeled by an electric circuit consisting of an ohmic resistance R_M accounting

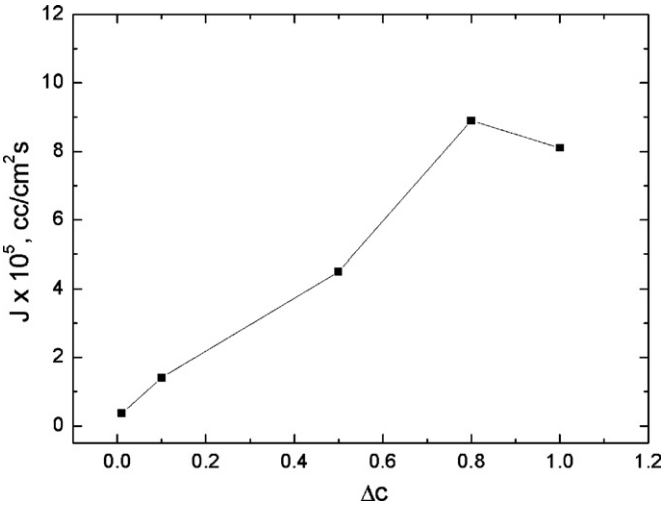

Fig. 4. Osmotic flux as a function of electrolyte concentration for the P5FNDIHS.

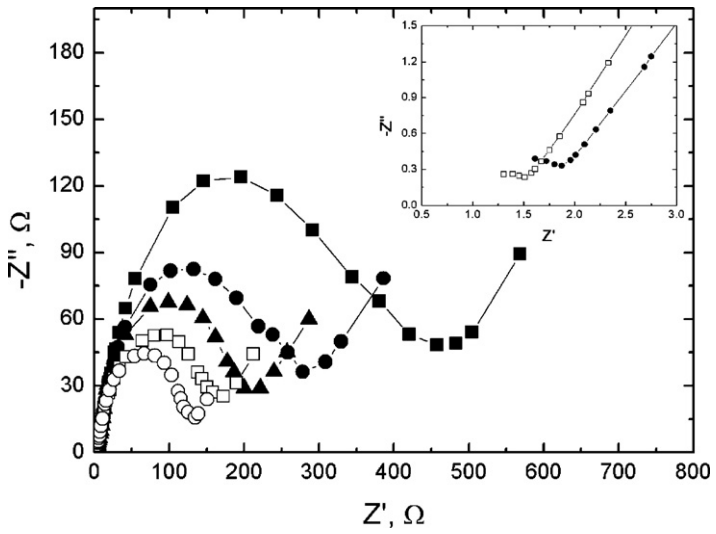

Fig. 5. Nyquist plots at 10 °C (■), 20 °C (●), 30 °C (▲), 40 °C (□) and 50 °C (○) for the P5FNDIHS membrane in the acid form equilibrated with distilled water. Inset: Zoom of the Nysquit plots at 20 °C and 40 °C in the high frequency region membrane.

for proton transport in the membrane in series with a parallel RC circuit. The RC circuit represents a Debye relaxation process with a single relaxation time $\tau = RC$. Strictly speaking, relaxation processes are described by a distribution of relaxation times and as a result it is more realistic to replace the capacitor by a constant phase element of admittance $Y*(\omega) = Y_0(j\omega\tau)^n$, $0 < n \leq 1$ [16]. The impedance of the circuit is given by

$$Z*(\omega) = R_M + \frac{R}{1 + Y_1(j\omega\tau)^n} \tag{6}$$

where $Y_1 = RY_0$ is a dimensionless parameter. The complex plane plot $Z''(\omega)$ vs. $Z'(\omega)$, called Nyquist diagram [17], is an arc intersecting the abscissa axis at $\omega \to \infty$ and $\omega \to 0$. Taking into account that $\lim_{\omega\to\infty} Z'(\omega) = R_M$ and $\lim_{\omega\to\infty} Z''(\omega) = 0$, the intersection of the arc with the abscissa axis at high frequencies gives the ohmic resistance of the membrane to proton transport. However, the Nyquist plot for the acidic P5FNDIHS membrane presented in Fig. 5 exhibits a more complex behavior at high frequencies. Actually the inset of the figure shows that at frequencies above that corresponding to the intersection of the loss impedance of the polarization curve with the abscissa axis the beginning of an arc appears which presumably intersects with the abscissa axis at the origin. As usual, the ohmic resistance of the membrane was taken as the impedance at the intersection of the extrapolated Z'' vs. Z' polarization curve with the abscissa axis in the high frequency region. On the other hand, the polarization arc in the low frequency region does not intersect with the abscissa axis as Eq. (6) predicts but both $|Z''|$ and Z' increase as frequency decreases. This behavior is presumably associated with a charge-transfer resistance R_{CT} and a double layer capacitance C_{dl}. The Warburg impedance [16,18,19] nearly always exhibits these two characteristics in such a way that it is conditioned by the diffusion of charges in the membrane–electrode interface. The value of this impedance for an interface of infinite thickness is given by

$$Z_W*(\omega) = \frac{\sigma}{\omega^{1/2}} - j\frac{\sigma}{\omega^{1/2}} \tag{7}$$

where σ is a constant that depends on $\Sigma_i(1/C_i^b D_i^{1/2})$ where C_i^b and D_i are, respectively, the bulk concentration and diffusion coefficients of the reactant species i. As a result the modulus of the impedance scales as $|Z_W{}^*(\omega)| \sim \omega^{-1/2}$, i.e. the double logarithmic plot of the modulus of the complex impedance is a straight line of slope $-1/2$ in the case of a double layer of infinite thickness. Although the results seem to support the existence of a Warburg impedance, there are not enough data in the low frequency region that allow to reach a definite conclusion concerning the membrane–electrode double layer thickness.

To account for the arc which presumably intersects with the abscissa axis at the origin, at high frequencies, the equivalent circuit of the membrane (ohmic resistance of the membrane in series with a circuit made up of constant phase element in parallel with the polarization resistance) should be in parallel with a capacitor, in the case of a semicircle, or a constant phase element for an arc. A scheme of the complete circuit is given in Fig. 6. At very high frequencies the contribution of the polarization to the impedance is negligible and the circuit representing the behavior of the membrane is the capacitor (constant phase element) in parallel with the resistance R_M of the membrane. At lower frequencies, the capacitance of the capacitor is infinite and the circuit formed by the polarization resistance in parallel with the constant phase element governs the behavior of the membrane. At very low frequencies the Warburg element describes the response of the membrane to the perturbation field.

An alternative method to determine the resistance of the membranes is the Bode diagram [20] consisting in the plot of both the modulus of the impedance and $\tan^{-1}(Z''/Z')$ against frequency. According to Eq. (6),

$$\lim_{\omega\to 0} \left|Z*(\omega)\right| = R_p + R_M; \quad \lim_{\omega\to\infty} \left|Z*(\omega)\right| = R_M \tag{8}$$

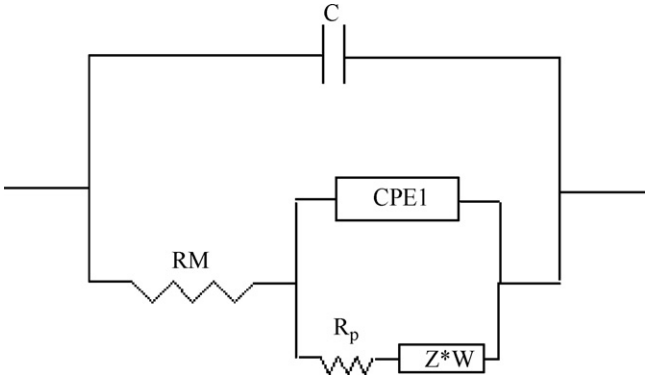

Fig. 6. Equivalent circuit of the membrane sandwiched by blocking electrodes.

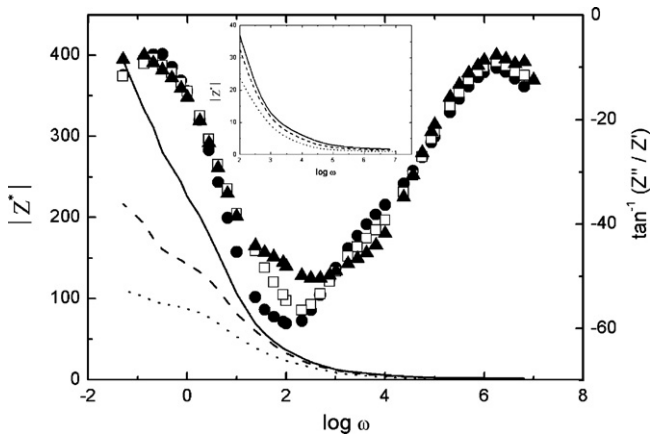

Fig. 7. Bode diagram showing the variation of the modulus of the impedance $|Z^*|$ (lines) and the out-of-phase angle $\phi = \tan^{-1}/(Z''/Z')$ (symbols) with the frequency at 20 °C (solid line and filled circles), 40 °C (dash line and open squares) and 60 °C (dot line and filled triangles) for the P5FNDIHS membrane in the acid form equilibrated with distilled water.

and

$$\phi = \lim_{\omega\to\infty}\tan^{-1}\left[\frac{Z''(\omega)}{Z'(\omega)}\right] = 0 \tag{9}$$

An illustrative Bode plot for the P5FNDIHS membrane is plotted in Fig. 7. The curves show that the modulus of the impedance undergoes a sharp decrease reaching a plateau whereas ϕ reaches a maximum at the plateau. The resistance of the membrane is taken as the value of $|Z*(\omega)|$ at the maximum of ϕ. It can be seen that at very high frequencies the modulus drops as a result of the fact that the capacitor in parallel with R_M in Fig. 6 governs the impedance of the circuit. The results obtained for R_M by the two methods are in rather good agreement. For example the value of R_M for the P5FNDIHS membrane at 30 °C estimated from Nyquist and Bode plots are respectively 1.79 and 1.70 Ω. For consistency, the results of the Bode plots obtained for R_M will be used in the analysis below.

The resistance R_M of the membrane was measured at different temperatures and the conductivity was obtained by means of the familiar expression

$$\sigma = \frac{l}{R_0 S} \tag{10}$$

where l and S are respectively thickness and area of the membrane in contact with the electrodes. The values of the conductivity obtained by the Nyquist and Bode plots are respectively 2.13 and 2.24 in S/m units. An illustrative Arrhenius plot showing the temperature dependence of the conductivity of the membrane obtained from the resistances of the membrane estimated from the Bode plot is shown in Fig. 8.

4. Discussion

Fig. 9 shows the representative morphology of the P5FNDIHS membrane. It is expected that the hydrophobic cyclopentane ring in the main chain and the pendant hydrophilic aromatic moieties are mutually incompatible and therefore segregations occur giving rise to sub-micron-sized domains observed in the AMF of P5FNDIHS. Moreover it is expected that the surface of the dry P5FNDIHS membrane has significant surface fluorine content compared to the theoretical bulky fluorine content owing to the low surface energy of the tetrafluorophenyl moieties which provide a thermodynamic driving force for the self-assembly at the surface air–polymer interface [21,22].

In spite of the high water uptake of the P5FNDIHS membrane, the moles of water per anionic fixed group in the membrane, λ,

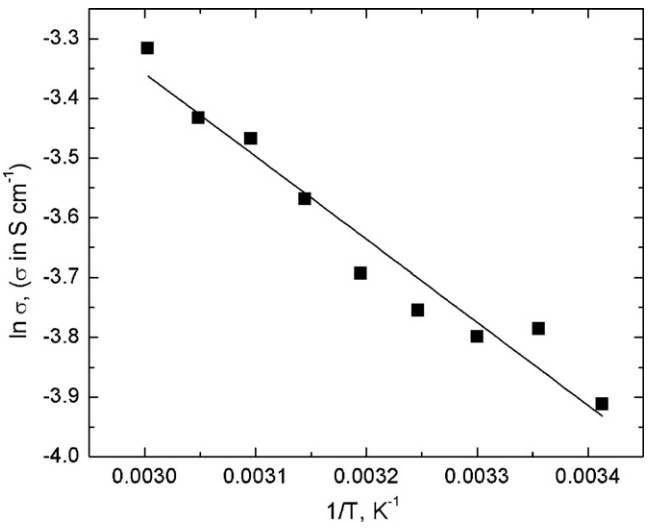

Fig. 8. Arrhenius plot showing the temperature dependence of the P5FNDIHS membrane.

is of the same order as that reported for Nafion [23] and copolyimide acid membranes [24,25]. It is worth noting in this regard that apparently dried naphthalenic polyimides may contain up to 10% of water. Moreover ^{1}H NMR experiments carried out on acidic naphthalenic polyimide membranes heated at 130 °C under vacuum show peaks at 0.7–1 ppm corresponding to water associated with imide groups [6]. This water may be absorbed by the membranes during the NMR experiments handling.

An inspection of the curves of Fig. 2 shows that a certain time that lies in the vicinity of 20,000 s is required in order that the *emf* of the concentration cell reaches a maximum. Then the *emf* slowly decreases as time increases. The value of the *emf* at the maximum was used to estimate the apparent transport number by means of Eq. (4). The curves presenting the variation of the transport number of protons with the geometrical average of the molality of the solutions flanking the membrane show that the

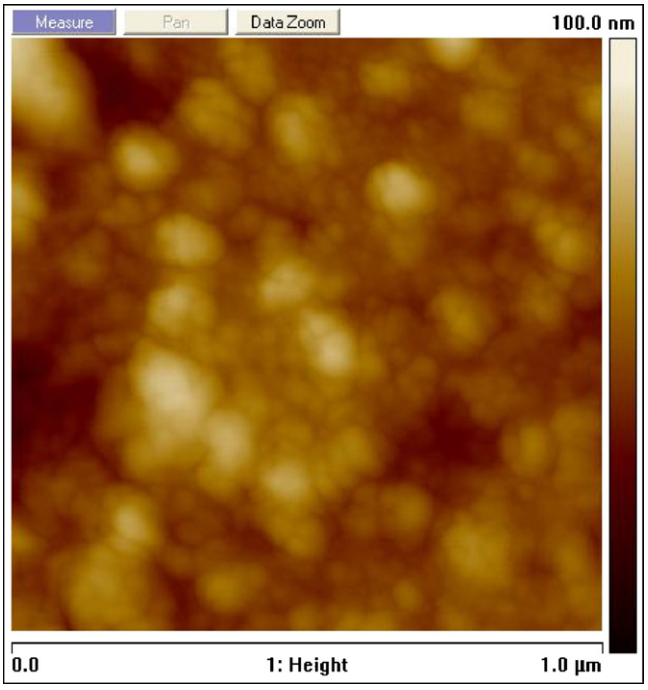

Fig. 9. AFM topographic image for the P5FNDIHS membrane.

membrane is ideally permselective for very dilute solutions, but the permselectivity undergoes a rather fast drop with increasing concentration. The drop of t_+ with increasing concentration for the P5FNDIHS membrane at long times, even for dilute concentration solutions suggests that the concentration of electrolyte equalizes in the two compartments of the concentration cell presumably as a consequence of strong electrolyte diffusion. To explain this behavior the membrane can be viewed formed by hydrophilic pores to the walls of which anionic SO_3^- groups are anchored. These groups prevent the diffusion of co-ions across the pores, and therefore hinder electrolyte diffusion thus increasing the transport number of counterions. The strong dependence of the counterion transport on electrolyte concentration suggests that the number of anionic fixed groups in the walls is not large enough to prevent co-ions diffusion across the membranes. As a result, electrolyte diffusion from the high to the low concentration compartment occurs, the c_2/c_1 ratio decreases and the electromotive force of the concentration goes down. Owing to the rather high time necessary to reach a maximum, and the rather high free ionic diffusion taking place in that period of time, the ratio a_2/a_1 presumably undergoes a significant decrease for the more concentrated solutions. Therefore, the *emf* at the maximum is the lower bound of this quantity and the transport number corresponding to the nominal values of c_2/c_1 should be higher than those obtained by means of Eq. (4).

In order to rationalize even further the *emf* results let us analyze the osmotic flow across the membrane, i.e. water flow from the distilled water compartment to the electrolyte compartment. Electrolyte transport from the solution compartment to the water compartment is in principle hindered by the fixed anions that exclude the chloride anions from the membrane, at least at very low concentrations. Water moves across the membrane under the driving force $d\mu_w/dx$, where μ_w is the chemical potential of water. Interactions with the surroundings giving by χu, where u is the velocity of water and χ the friction coefficient water-surroundings, opposes to the displacement of water. In steady state conditions $\chi u + d\mu_w/dx = 0$, so that $u = -(1/\chi)d\mu_w/dx$. The flux of water across the membrane is $J_w = uc_w$ where c_w is the concentration of water in the membrane phase. Taking into account that for very dilute solutions ($c \to 0$), $\mu_w = \mu_w^0 + RT\ln x_w \cong \mu_0 + RTx$, where x_w and x are respectively the molar fraction of water and HCl in the solution it is found that $J_w \cong (RTc_w/\chi)(x/l)$. In these circumstances the flux of water is given by

$$J_w \cong iD_w\frac{c}{l} \tag{11}$$

where use of the Einstein's relationship between friction coefficient and diffusion coefficient ($D = RT/\chi$) was used. In Eq. (11), l and c represent respectively the thickness of the membrane and the concentration of the solution. Strictly speaking, instead of c the activity coefficient of the solution should be used. Moreover $i = 2$ for very dilute solutions and lower than 2 for higher concentrations. Following this approach, the diffusion coefficient of water for the HCl 0.01 N solution is 1.8×10^{-8} m^2/s. This result is nearly one order of magnitude higher than the self-diffusion coefficient of water measured by H^+ NMR spectroscopy in distilled water which amounts to 2.2×10^{-9} m^2/s at room temperature [26–28]. Since friction of the diffusing water with the membrane matrix should decrease the motion of the diffusive water molecules, the results found for D_w from osmotic measurements at very low concentrations are overestimated. This is due to the fact that under the driving force of the chemical potential of the electrolyte protons in the solution migrate to the side of the membrane facing the water compartment. Because fixed ions in the membrane hinder chloride anions transport across the membrane, the side of the membrane in contact with the solution is negatively charged whereas that in contact with distilled water is positively charged. As a result an electric potential is created inside the membrane that drags the pore liquid positively charged toward the solution compartment, enhancing the osmotic flow. Therefore the driving forces in the osmotic flow are the chemical potential of water and the electric potential created inside the membrane. As the concentration of the solution increases, chloride anions are not totally rejected by the fixed anions of the membrane and diffusion of hydrochloric acid from the concentration compartment to the distilled water compartment occurs. However, this migration does not eliminate the electric potential created inside the membrane and the osmotic flow is still higher than that caused by the gradient of chemical potential of water. Both ionic transport and osmotic flow tend to decrease the c_2/c_1 ratio, and the value of this quantity decreases as time increases. In view of these facts not only the ionic diffusion across the membrane to which we have alluded before but also osmotic flow may be responsible for the decrease occurring at long times in the *emf* of the concentration cells.

The conductivity of membranes can be obtained in the plane of the membrane (in-plane, longitudinal or transverse directions) and through the thickness of the membrane (through-plane). The former technique may be more useful than the latter in the case of the conductivity of anisotropic membranes, whereas the latter is better for membranes used in low temperature fuel cells. However, the values of the conductivities obtained by both techniques coincide for isotropic membranes like those studied in this work [29]. The conductivity of the P5FNDIHS membrane obtained in this study using the through plane technique was 2.24 S/m, at 30 °C, of the same order of that reported for high conductivity acidic membranes [30]. An Arrhenius plot representing the temperature dependence of the membrane, presented in Fig. 8, shows that the activation energy associated with proton transport across the membrane is only 2.8 ± 0.2 kcal/mol.

The study of the mechanism governing proton transport in acidic ion-exchange membranes has drawn the attention of many researchers [31,32]. Ab initio simulations suggest that the proton state in bulk water and in water clusters fluctuates between more localized hydronium ion-like states or Eigen ions and more delocalized $H_5O_2^+$-like states or Zundel ions in such a way that forming and breaking hydrogen bonds in the neighborhood of the proton location (Grotthus like hoping) may be responsible for proton transport [33–37]. Proton diffusion involving this mechanism presumably takes place in high conductivity membranes, such as the P5FNDIHS membrane, is named structural diffusion. In low conductivity membranes water acts as a carrier of protons and the transport is called vehicular diffusion.

It is tempting to compare the diffusion of water in the P5FNDIHS membrane with that of protons, the latter obtained from the proton conductivity using Nernst–Planck type equations. Let us consider the electric current inside the acidic membranes as a result of the motions of protons in the membrane under an electric potential gradient driving force, $-d\psi/dx$. In steady state conditions the velocity of the protons is $u = -(F/\chi)(d\psi/dx)$ where F is Faraday's constant and χ is the friction coefficient which is related to the diffusion coefficient of protons by the Einstein's relationship indicated above. Taking into account that the density of current in the membrane equilibrated with water is $i = FJ(H^+) = F^2c(H^+)(D/RT)](-d\psi/dx)$, $D(H^+)$ is obtained as

$$D(H^+) = \frac{RT\sigma}{F^2c(H^+)} \tag{12}$$

where $\sigma = i/(-d\psi/dx)$. By taking as $c(H^+)$ the average of the IECs obtained by titration and NMR, the values of $D(H^+)$ for the P5FNDIHS membrane at 30 °C is 4.09×10^{-10} m^2/s. The value of $D(H^+)$ for the P5FNDIHS membrane is nearly two order of magnitude lower than that obtained for $D(H_2O)$ by osmotic measurements at very low concentrations. In general the diffusion

coefficient of protons in fully hydrated high conductive membranes, such as the P5FNDIHS membrane, is much higher than the self-diffusion coefficient of water in the membrane phase. Only for low conductivity membranes $D(H^+)$ is similar to the self-diffusion coefficient of water [6]. Therefore the comparative results between $D(H^+)$ and $D(H_2O)$ obtained by Eq. (11) put in evidence the high contribution to the osmotic flow of the internal electric potential created between the two faces of membrane by effect of the hydrochloric acid solution gradient.

5. Conclusions

In spite of the bulkiness of the functionalized norbornene structural units, efficient segregation of hydrophilic from hydrophobic moieties, presumably favored by the low polarity of C^{ar}—F bonds attached to the phenyl groups, give rise to the formation of percolation paths responsible for the rather high proton conductivity of the polymeric membrane. The performance of this membrane in this regard is similar to that of other membranes used in low temperature fuel cells.

The electromotive force of the concentration cells undergoes a decrease at long times in the polymeric membrane. Enhanced osmotic flow by effect of the internal potential membrane arising from protons migration to the side of the membrane facing the dilute solution, in conjunction with free-electrolyte diffusion are responsible for the diminution of the c_2/c_1 ratio and as a result of the decrease of the *emf* of the concentration cells.

Acknowledgements

Financial support from National Council for Science and Technology of Mexico (CONACYT) (PhD Scholarship to A.A.S.) is gratefully acknowledged. We thank CONACYT-SEMARNAT and ICyTDF for generous support with contracts 23432 and 4312. We are grateful to Alejandrina Acosta, Carlos Flores Morales and Miguel Ángel Canseco for their assistance in NMR, AFM and thermal properties, respectively. This work was also supported by the CICYT through the project MAT2008-06725-C03-01.

References

[1] T. Sata, Ion-Exchange Membranes, RSC, Cambridge, 2004.
[2] T. Xu, Ion exchange membranes: state of their development and perspective, J. Membr. Sci. 263 (2005) 1–29.
[3] S. Cui, J. Liu, M.E. Selvan, D.J. Keffer, B.J. Edwards, W.V. Steele, A molecular dynamics study of a Nafion polyelectrolyte membrane and the aqueous phase structure for proton transport, J. Phys. Chem. B 111 (2007) 2208–2218.
[4] J. Ennari, M. Elomaa, F. Sundholm, Modelling a polyelectrolyte system in water to estimate the ion-conductivity, Polymer 40 (1999) 5035–5041.
[5] J. Pozuelo, E. Riande, E. Saiz, V. Compañ, Molecular dynamics simulations of proton conduction in sulfonated poly (phenyl sulfone)s, Macromolecules 39 (2006) 8862–8866.
[6] L. Garrido, J. Pozuelo, M. López-González, J. Fang, E. Riande, Simulation and experimental studies of proton diffusion in polyelectrolytes based on sulfonated naphthalenic copolyimides, Macromolecules 42 (2009) 6572–6580.
[7] M.A. Hickner, H. Ghassemi, Y.S. Kim, B.R. Einsla, J.E. McGrath, Alternative polymer systems for proton exchange membranes (PEM)s, Chem. Rev. 104 (2004) 4587–4612.
[8] A.P. Contreras, M.A. Tlenkopatchev, M.M. López-González, E. Riande, Synthesis and gas transport properties of new high glass transition temperature ring-opened polynorbornenes, Macromolecules 35 (2002) 4677–4684.
[9] M. Tlenkopatchev, J. Vargas, M.A. Almaráz-Girón, M. López-González, E. Riande, Gas sorption in new fluorine containing polynorbornenes with imide side chain groups, Macromolecules 38 (2005) 2696–2703.
[10] J. Vargas, A.A. Santiago, M.A. Tlenkopatchev, M. López-González, E. Riande, Gas transport in membranes based on polynorbornenes with fluorinated dicarboximide side moieties, J. Membr. Sci. 361 (2010) 78–88.
[11] J. Vargas, A.A. Santiago, M.A. Tlenkopatchev, R. Gaviño, M. Fe Laguna, M. López-González, E. Riande, Gas transport and ionic transport in membranes based on polynorbornenes with functionalized imide side groups, Macromolecules 40 (2007) 563–570.
[12] A.A. Santiago, J. Vargas, S. Fomine, R. Gaviño, M.A. Tlenkopatchev, Polynorbornene with pentafluorophenyl imide side chain groups: synthesis and sulfonation, J. Polym. Sci. A: Polym. Chem. 48 (2010) 2925–2933.
[13] D. O'Hagan, Understanding organofluorine chemistry. An introduction to the C—F bond, Chem. Soc. Rev. 37 (2008) 308–319.
[14] Y.P. Yampoĺskii, N.B. Bespalova, E. Sh Finkeĺshtein, V.I. Bondar, A.V. Popov, Synthesis, gas permeability, and gas sorption properties of fluorine-containing norbornene polymers, Macromolecules 27 (1994) 2872–2878.
[15] V. Compañ, F.J. Fernández-Carretero, E. Riande, A. Linares, J.L. Acosta, Electrochemical properties of ion-exchange membranes based on sulfonated EPDM-polypropylene blends, J. Electrochem. Soc. 154 (2007) B159–B164.
[16] E. Barsoukov, J.R. Macdonalds, Impedance Spectroscopy: Theory, Experiment and Applications, 2nd ed., Wiley, NJ, 2005 (Chapter 2).
[17] H. Nyquist, Thermal agitation of electric charge in conductors, Phys. Rev. 32 (1928) 110–113.
[18] E. Warburg, About the behaviour of so-called impolarizable electrodes in the presence of alternating current, Ann. Phys. Chem. 67 (1899) 493–499.
[19] A.J. Bard, L.R. Faulkner, Electrochemical Methods. Fundamentals and Applications, 2nd ed., Wiley, 2001 (Section 10.3).
[20] W.W. Bode, Network Analysis in Feedback Amplifier Design, Van Nostrand, Princenton, NJ, 1956.
[21] S. Wu, Polymer Interface and Adhesion, Marcel Dekker, New York, 1982 (Chapter 5).
[22] H. Ghassemi, J.E. McGrath, T.A. Zawodzinsky Jr., Multiblock sulfonated-fluorinated poly(arylene ether)s for a proton exchange membrane fuel cell, Polymer 47 (2006) 4132–4139.
[23] R. O'Hayre, S.-W. Cha, W. Colella, F.B. Prinz, Fuel Cell Fundamentals, Wiley & Sons, New York, 2006 (Chapter 4).
[24] X. Guo, F. Zhai, J. Fang, M.F. Laguna, M. López-González, E. Riande, Permselectivity and conductivity of membranes based on sulfonated naphthalenic copolyimides, J. Phys. Chem. B 111 (2007) 13694–13702.
[25] S. Yuan, C. del Rio, M. López-González, X. Guo, J. Fang, E. Riande, Impedance spectroscopy and performance of cross-linked new naphthalenic polyimide acid membranes, J. Phys. Chem. C 114 (2010) 22773–22782.
[26] K.R. Harris, P.J. Newit, Self-diffusion of water at low temperatures and high pressure, J. Chem. Eng. Data 42 (1997) 346–348.
[27] K. Krynicki, C.D. Green, D.W. Sawyer, Pressure and temperature dependence of self-diffusion in water, Faraday Dis. Chem. Soc. 66 (1978) 199–208.
[28] K.R. Harris, L.A. Woolf, J. Chem. Soc. Faraday Trans. I 76 (1980) 377–385.
[29] K.R. Cooper, Characterization through-plane and in-plane ionic conductivity of polymer electrolyte membranes, ECS Trans. 41 (2011) 1371–1380.
[30] M. Rikukawa, K. Sanui, Proton conducting polymer electrolyte membranes based on hydrocarbon polymers, Prog. Polym. Sci. 25 (2000) 1463–1502.
[31] S.J. Paddison, Proton conduction mechanisms at low degrees of hydration in sulfonic acid-based polymer electrolytes membranes, Annu. Rev. Mater. Res. 33 (2003) 289–319.
[32] K.D. Kreuer, S.J. Paddison, E. Spohr, M. Schuster, Transport in proton conductors for fuel cell applications: simulations, elementary reactions, and phenomenology, Chem. Rev. 104 (2004) 4637–4678.
[33] M. Tuckerman, K. Laasonen, M. Sprik, M. Parrinello, Ab initio molecular dynamics simulation of the solvation and transport of hydronium and hydroxyl ions in water, J. Chem. Phys. 103 (1995) 150–161.
[34] M. Tuckerman, K. Laasonen, M. Sprik, M. Parrinello, Ab initio molecular dynamics simulation of the solvation and transport of $H3O^+$ and OH^- ions in water, J. Phys. Chem. 99 (1995) 5749–5752.
[35] M.E. Tuckerman, D. Marx, M. Klein, M. Parrinello, On the quantum nature of the shared proton in hydrogen bonds, Science 275 (1997) 817–820.
[36] D. Marx, M.E. Tuckerman, J. Hutter, M. Parrinello, The nature of the hydrated excess proton in water, Nature 397 (1999) 601–604.
[37] D. Marx, M.E. Tuckerman, M. Parrinello, Solvated excess protons in water: quantum effects on the hydration structure, J. Phys. Condens. Matter 12 (2000) A153–A159.